Archives of Oral Biology 127 (2021) 105136

Contents lists available at ScienceDirect

Archives of Oral Biology

journal homepage: www.elsevier.com/locate/archoralbio

Histology of human teeth: Standard and specific staining methods revisited

M. Widbiller [a,*], C. Rothmaier [a], D. Saliter [a], M. Wölflick [a], A. Rosendahl [a], W. Buchalla [a], G. Schmalz [b], T. Spruss [c], K.M. Galler [a]

[a] Department of Conservative Dentistry and Periodontology, University Hospital Regensburg, Regensburg, Germany
[b] Department of Periodontology, University of Bern, Bern, Switzerland
[c] Central Animal Facilities, University of Regensburg, Regensburg, Germany

ARTICLE INFO

Keywords:
Fixatives
Formaldehyde
Histological techniques
Nerve tissue
Dental pulp

ABSTRACT

Objective: Histological techniques have long been an integral part of dental research. Especially the processing of complex tissues poses specific challenges, however, literature offers only few technical references. Objectives of this study were therefore to optimize histological staining methods and compile detailed protocols for preparation and staining of dental tissues.

Methods: Human teeth were collected and fixed with 4 % formaldehyde solution after extraction. Subsequently, teeth were decalcified in 17 % EDTA or Morse's solution over a period of 28 days. The extent of decalcification was determined by weight loss and radiography.

After sectioning, histological staining methods were optimized for their use on teeth. These included hematoxylin-eosin, Masson trichrome, Masson-Goldner trichrome and May-Gruenwald-Giemsa staining. Nerve fibres were visualized by luxol fast blue staining and Bodian silver staining. In addition, specific methods like TRAP, modified Brown and Brenn as well as picrosirius red staining with light polarization or fluorescence were applied and optimized.

Results: Preparation of an artificial access to the pulp chamber was essential to ensure prompt penetration of the chemicals. Decalcification with Morse's solution took at least two weeks but was more efficient than 17 % ETDA, where thorough demineralization was achieved only after three weeks. The staining methods exhibited differences not only regarding their ability to display specific structures of interest, but also in terms of reproducibility.

Conclusion: High-quality histology of teeth can only be achieved after optimal tissue preparation and accurate staining. A complementary use of staining techniques is necessary to answer specific research questions.

1. Introduction

More than 300 years ago, in 1677, the Dutch scientist Antonie van Leeuwenhoek published his famous paper 'letter on the protozoa'. By using the single-lens microscopes he had manufactured by his own hand, he was able to give a detailed description of protists and bacteria that live around humans, e.g. in the oral cavity, for the first time (Gest, 2004; Lane, 2015). The technical capability to produce magnifying lenses formed the basis for the development of histological methods to study the microscopic anatomy of various biological tissues. With their roots in the 17th century, histological staining techniques became increasingly important and still are an inherent part of medical diagnostics and research (Bracegirdle, 1977). In the early days, the main purpose of histological analyses was to gain insight in the microanatomy of different tissues and thus to be able to draw conclusions about their physiological functions. A milestone was Camillo Golgi's description of nervous tissue at the end of the 19th century; he had succeeded in visualizing the arborization of dendrites and branching of axons using a silver nitrate impregnation technique. This visualization of the architecture and complexity of nerve tissues formed a basis for modern neuroscience (Mazzarello et al., 2009). In the course of time, the histological diagnostics and classification of tissue pathologies became routinely performed medical procedures. Besides the continuous technical improvement of microscopes, a striking progress was the development of immunohistochemistry in the 1980s, which revolutionized both biological research and medical diagnostics, e.g. by antibody-based identification of cancer cells (Musumeci, 2014).

Histological methods have also offered unique opportunities in

* Corresponding author at: Department of Conservative Dentistry and Periodontology, University Hospital Regensburg, Franz-Josef-Strauß-Allee 11, D-93053 Regensburg, Germany.
E-mail address: matthias.widbiller@ukr.de (M. Widbiller).

https://doi.org/10.1016/j.archoralbio.2021.105136
Received 30 December 2020; Received in revised form 1 April 2021; Accepted 23 April 2021
Available online 29 April 2021

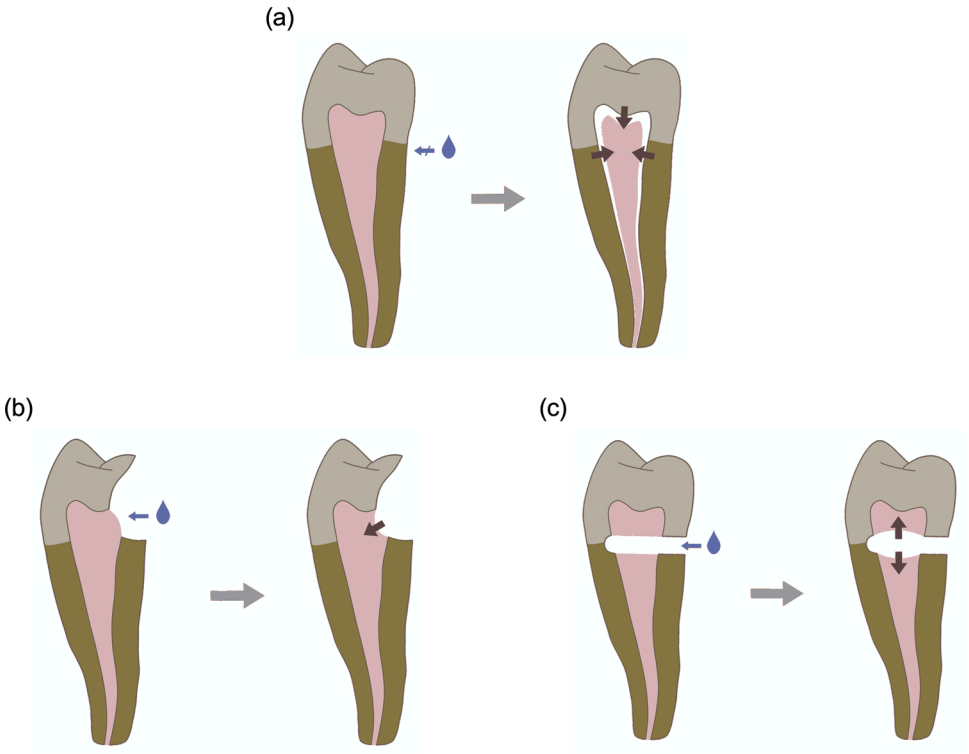

Fig. 1. Preparation of teeth prior to fixation. (a) The penetration of the fixative into the pulp is limited due to the mineralized tissue mantle. Furthermore, concentric contraction of pulp tissue leads to extensive detachment from the dentine walls, which results in an artificial gap between pulp tissue and dentine. (b) Drilling an access at a non-relevant area improves penetration of the fixative into the pulp and enables a directed contraction. (c) Separation of the crown from the root maximizes penetration of fixating fluids, and soft tissue can contract towards the respective dentine area, which results in improved quality and allows for analysis of crown and root of the same specimen in position.

dental research. The microscopic visualization of teeth made it possible to describe all the anatomical structures of a tooth in detail, among them the dental pulp, a connective tissue that is enclosed by the mineralized enamel, dentine and cementum. The pulp's various cell types and structures of the peripheral nervous system as well as their responses to external stimulation have been subject to numerous investigations over the last years (Couve et al., 2013; Couve et al., 2018; Ricucci et al., 2017). Furthermore, histological techniques facilitated the evaluation of standard clinical diagnostic methods to assess the pulpal status such as percussion and sensibility testing. In this context, Ricucci et al. demonstrated recently that clinical diagnoses are not always consistent with the corresponding histological observations, which has initiated considerations to make adjustments to the clinical nomenclature of pulpal inflammation (Ricucci et al., 2014; Wolters et al., 2017). Histological imaging can furthermore confirm the validity of already existing but also of new therapeutic methods. In this context, sophisticated techniques such as fluorescence aided caries excavation (FACE) as an effective method to distinguish carious from sound dentine found its application in clinical dentistry (Lennon et al., 2006). Histology has thus been an indispensable method in the field of dental research and still is today.

Dental tissues pose particular challenges to the experimenter striving for high-quality histologic preparations due to the close proximity of various different soft and mineralized tissues. Therefore, standard histological procedures had to be modified accordingly. In general, a rapid fixation is necessary to preserve the tissues' anatomical structure. With teeth, challenges arise concerning the diffusion of the fixation fluid through the mantle of hard tissue around the soft core. Only quick and sufficient penetration prevents rapidly progressing decay and autolysis of the pulp tissue and enables the representation of specimens without artefacts (Willman, 1937). Subsequently, teeth as 'composite samples' have to be demineralized and dehydrated gently enough to limit potential damage. After embedding in paraffin, the specimens can be manually sectioned on a microtome, mounted on microscope slides and stained (Slaoui & Fiette, 2011). A comparative description of adequate sample preparation of dental tissues is not to be found in the literature and accurate technical details on fixation and decalcification are mostly missing.

Despite the fact that multiple histological techniques are well-established, respective protocols rarely refer to the complex dental tissues or report methodical details. In the past, classical as well as specific staining protocols, e.g. for the visualization of nerve fibres or for enzyme histochemical methods, have been applied to dental tissues without commenting on methodical challenges (Langeland, 1987; England et al., 1974; Katele & James, 1962; Fuenzalida et al., 1999; Pereira et al., 2014).

Therefore, the aim of this study was to define the parameters of optimal preparation of dental tissues and to provide a compilation of optimized and detailed protocols for classical but also for specific or innovative histological techniques to fellow researchers.

2. Materials and methods

Detailed information on the chemicals and reagents used can be found in the Supplementary data.

2.1. Fixation and demineralization

Freshly extracted teeth were fixed in 4 % formaldehyde solution at room temperature for at least 24 h. In order to ensure sufficient penetration of fixatives into the pulpal tissue, two different preparation techniques to expose the pulp were tested in preliminary experiments (Fig. 1a–c). The first approach was to create a small access through enamel and dentine with a diamond bur outside the area of interest (Fig. 1b). In a second approach, the crown was partially separated from the root with a diamond bur, retaining a segment of dentine to keep both segments attached, which kept the segments fixed in exact position to each other (Fig. 1c).

To find the optimal decalcifying agent, 16 single-rooted and 16 multi-rooted teeth were collected and randomly distributed into 2 groups by coin toss. Teeth were demineralized either by Morse's solution, an aqueous solution of 22.5 % formic acid and 10 % sodium citrate,

or 17 % EDTA solution. The mineral loss was evaluated by gravimetric analysis (Quintix® Analytical Balance, Sartorius, Göttingen, Germany) and standardized X-rays (0.05 s and 60 kV; Heliodent^{PLUS}, Sirona Dental Systems, Wals, Austria) once a week. Each tooth was demineralized in a volume of 100 mL, the demineralizing agent was changed weekly ($n = 8$). The initial and final weights were set to 100 % and 0 % respectively, and medians with 25–75 % percentiles were calculated. A curve was fit to visualize the time course of demineralization [Y = (Y0 - Plateau) * exp (-K*X) + Plateau] and to calculate the half-life [ln(2)/K]. Data were analysed non-parametrically by means of Mann-Whitney *U*-Tests on a $\alpha = 0.05$ level of significance (GraphPad Prism 9; GraphPad Software, La Jolla, CA).

Demineralized samples for histological staining were washed in distilled water (2 × 20 min), dehydrated in ascending concentrations of ethanol (2 × 30 min 70 %, 30 min 90 %, 2 × 30 min 96 %, 30 min 100 %, 45 min 100 %) and cleared in xylene (2 × 60 min).

Dehydrated teeth were immersed in molten paraffin (56 °C) over night and embedded in the same material. Consecutive sections of 4 μm thickness (Rotary Microtome A550, MEDITE Medical, Burgdorf, Germany) were mounted to microscope slides (SuperFrost Plus™ Adhesion slides, Thermo Fisher Scientific, Waltham, MA, USA). After staining, the samples were covered with an appropriate mounting medium, which will be specified below, and cover slips (Cover slips, Carl Roth, Karlsruhe).

2.2. Hematoxylin-eosin staining

2.2.1. Solutions and reagents

- Hemalaun solution acid according to Mayer
- Eosin Y solution 1 % (freshly filtered) + acetic acid (4 drops per 250 mL)

2.2.2. Procedure

1 Dewax (2 × 15 min xylene) and hydrate in descending concentrations of ethanol (2 × 5 min 100 %, 5 min 96 %, 5 min 90 %, 2 × 5 min 70 %, distilled water)
2 Stain in freshly filtered hemalaun solution for 10–20 min (time has to be extended in case of repeated use of solution)
3 Wash in lukewarm running tap water for 5 min
4 Stain in eosin solution for 1 min
5 Dehydrate in ascending concentrations of ethanol (2 × 2 min 70 %, 2 min 90 %, 2 min 96 %, 2 × 2 min 100 %)
6 Clear in xylene (2 × 10 min) and mount in resinous medium (e.g. entellan)

2.3. Masson trichrome staining

2.3.1. Solutions and reagents

- Bouin's solution
- Hematoxylin solutions A and B according to Weigert (1 part solution A + 1 part solution B)
- Biebrich scarlet-acid fuchsin solution
- Phosphomolybdic acid solution and phosphotungstic acid solution (1 part of each acid solution + 2 parts distilled water)
- Acetic acid, 1 % aqueous solution
- Aniline blue solution

2.3.2. Procedure

1 Dewax (2 × 15 min xylene) and hydrate in descending concentrations of ethanol (2 × 5 min 100 %, 5 min 96 %, 5 min 90 %, 2 × 5 min 70 %, distilled water)
2 Incubate for 15 min at 56 °C in Bouin's solution (alternative: overnight at room temperature)
3 Wash in lukewarm running tap water until yellow color is removed
4 Stain in freshly filtered hematoxylin solution for 5 min
5 Wash in lukewarm running tap water for 5 min
6 Rinse with distilled water
7 Stain in freshly filtered Biebrich scarlet-acid fuchsin solution for 4 min
8 Rinse in three changing baths of distilled water
9 Place in phosphomolybdic/tungstic acid solution for 5 min
10 Stain in freshly filtered aniline blue solution for 5 min
11 Dip in 1 % acetic acid solution
12 Place in 1 % acetic acid solution for 2 min
13 Rinse with distilled water
14 Dehydrate in ascending concentrations of ethanol (2 × 2 min 70 %, 2 min 90 %, 2 min 96 %, 2 × 2 min 100 %)
15 Clear in xylene (2 × 10 min) and mount in resinous medium (e.g. entellan)

2.4. Masson-Goldner trichrome staining

2.4.1. Solutions and reagents

- Hematoxylin solutions A and B according to Weigert (1 part solution A + 1 part solution B)
- Acid fuchsine - ponceau azophloxine
- Phosphomolybdic acid - orange G (A)
- Acetic acid, 1 % aqueous solution
- Light green 0.2 %

2.4.2. Procedure

1 Dewax (2 × 15 min xylene) and hydrate in descending concentrations of ethanol (2 × 5 min 100 %, 5 min 96 %, 5 min 90 %, 2 × 5 min 70 %, distilled water)
2 Stain in freshly filtered hematoxylin solution for 30 min
3 Rinse with distilled water for 15 s
4 Wash in lukewarm running tap water for 3 min
5 Stain in acid fuchsine - ponceau azophloxine solution for 8 min
6 Place in 1 % acetic acid solution for 10 s
7 Stain in freshly filtered phosphomolybdic acid - orange G solution for 40 min
8 Place in 1 % acetic acid solution for 10 s
9 Stain in light green 0.2 % solution for 8 min
10 Place in 1 % acetic acid solution for 30 s
11 Wash in lukewarm running tap water for 1 min
12 Dehydrate in ascending concentrations of ethanol (2 min 90 %, 2 min 96 %) and isopropanol for 2 min
13 Clear in xylene (2 × 15 min) and mount in resinous medium (e.g. entellan)

2.5. Tartrate-resistant acid phosphatase (TRAP) staining

It should be noted that this staining technique requires demineralization in EDTA solution.

2.5.1. Solutions and reagents

- Hemalaun solution acid according to Mayer
- TRAP staining solution (40 mg naphthol AS-MX phosphate disodium salt, 4 mL *N,N*-dimethylformamide, 240 mg fast red violet LB salt, 2 mL triton X, 200 mL TRAP buffer)
- TRAP buffer (1.64 g sodium acetate + 23.005 g disodium tartrate dihydrate, dilute in 300 mL aqua dest., adjust pH-value to 5 using HCl, fill up to 500 mL)

2.5.2. Procedure

1 Dewax (2 × 15 min xylene) and hydrate in descending concentrations of ethanol (5 min 100 %, 5 min 96 %, 5 min 70 %, distilled water)
2 Place in TRAP buffer for 10 min
3 Stain in TRAP staining solution for 4 h at 37 °C
4 Rinse with distilled water
5 Stain in freshly filtered hemalaun solution for 2–3 min (time has to be extended in case of repeated use of solution)
6 Wash in lukewarm running tap water for 5 min
7 Mount in aquatex immediately

2.6. Picrosirius red staining

2.6.1. Solutions and reagents

- Hematoxylin solutions A and B according to Weigert (1 part solution A + 1 part solution B)
- Sirius red (direct red), 0.1 % solution in saturated aqueous solution of picric acid
- Acetic acid, 0.5 % aqueous solution

2.6.2. Procedure

1 Dewax (2 × 15 min xylene) and hydrate in descending concentrations of ethanol (2 × 5 min 100 %, 5 min 96 %, 5 min 90 %, 2 × 5 min 70 %, distilled water)
2 Stain in freshly filtered hematoxylin solution for 8 min
3 Wash in lukewarm running tap water for 10 min
4 Stain in freshly filtered picrosirius red solution for 60 min
5 Rinse in two changing baths of 0.5 % acetic acid solution
6 Remove most of the solution by shaking
7 Dehydrate in 3 changing baths of 100 % ethanol
8 Clear in xylene (2 × 10 min) and mount in resinous medium (e.g. entellan)

2.7. Modified Brown and Brenn staining

2.7.1. Solutions and reagents

- Crystal violet, 1 % aqueous solution
- Iodine-potassium iodide solution according to Lugol
- Fuchsine basic, 0.25 % aqueous solution
- Picric acid (aqueous saturated), 10 % acetone solution
- Acetone-ethanol mixture (1 part acetone + 1 part ethanol)

2.7.2. Procedure

1 Staining a tissue sample infected with bacteria as a positive control has proven to be essential.
2 Dewax (2 × 15 min xylene) and hydrate in descending concentrations of ethanol (2 × 5 min 100 %, 5 min 96 %, 5 min 90 %, 2 × 5 min 70 %, distilled water)
3 Stain with freshly filtered crystal violet solution for 3 min
4 Rinse with distilled water
5 Place in freshly filtered iodine-potassium iodide solution for 1 min
6 Rinse with distilled water
7 Differentiation: decolorize in acetone-ethanol mixture for ca. 30 s, move carefully to remove excess stain
8 Rinse with distilled water
9 Stain with basic fuchsine solution for 3 min
10 Rinse with distilled water
11 Place in picric acid solution for ca. 20 s, move carefully to remove excess stain
12 Dehydrate in 3 changing baths of 100 % ethanol
13 Clear in xylene (2 × 10 min) and mount in resinous medium (e.g entellan)

2.8. May-Gruenwald-Giemsa staining

2.8.1. Solutions and reagents

- May-Gruenwald solution (1 part stock solution + 1 part Sorensen's phosphate buffer)
- Giemsa solution (1 part stock solution + 9 parts Sorensen's phosphate buffer)
- Sorensen's phosphate buffer 0.1 M, pH-value adjusted to 6.9

2.8.2. Procedure

1 Dewax (2 × 15 min xylene) and hydrate in descending concentrations of ethanol (2 × 5 min 100 %, 5 min 96 %, 5 min 90 %, 2 × 5 min 70 %, distilled water)
2 Remove most of the water by shaking
3 Place in methanol for at least 10 min
4 Stain in freshly filtered May-Gruenwald solution for 7 min
5 Drain staining solution
6 Stain in freshly filtered Giemsa solution for 20 min
7 Rinse with Sorensen's phosphate buffer
8 Wash in Sorensen's phosphate buffer for 30 s
9 Air-dry sections completely
10 Clear in xylene (2 × 10 min) and mount in resinous medium (e.g entellan)

2.9. Luxol fast blue staining

2.9.1. Solutions and reagents

- Luxol fast blue
- Papanicolaou's solution 1a (S) (also known as Harris hematoxylin)
- Lithium carbonate, 0.05 % aqueous solution

2.9.2. Procedure

1 Dewax (2 × 15 min xylene) and place in 2-propanol for 4 min
2 Place in 96 % ethanol for 4 min twice
3 Stain in freshly filtered luxol fast blue for 12 h or overnight at 60 °C
4 Wash in 96 % ethanol for 10 s
5 Rinse with distilled water for 10 s
6 Dip in lithium carbonate solution for 5 s
7 Differentiate in 70 % ethanol for 30 s
8 Rinse with distilled water for 10 s
9 Place in lithium carbonate solution for 30 s
10 Dip in 70 % ethanol for 5 s
11 Rinse with distilled water for 30 s
12 Stain in freshly filtered hematoxylin solution for 2 min
13 Wash in lukewarm running tap water for 5 min
14 Dehydrate in 96 % ethanol solution (2 × 4 min) and isopropanol for 4 min
15 Clear in xylene (2 × 10 min) and mount in resinous medium (e.g entellan)

2.10. Bodian silver staining

2.10.1. Solutions and reagents

- Protargol S, 1 % aqueous solution, dissolve at 55 °C with copper sheet (0.7 mm, 60 × 80 mm) in the cuvette
- Hydrochinon, 1 % aqueous solution

Table 1
Filter used for fluorescence imaging.

	ZEISS filter set	Excitation	Beamsplitter	Emission
Green	38	BP 470/40	FT 495	BP 525/50
Red	43	BP 545/25	FT 570	BP 605/70

BP = band pass; transmission peak/band width at half maximum [nm].

- Intensifier: silver nitrate 5 % (38 mL) + stock solution B (162 mL)
- Gold chloride, 0.1 % aqueous solution + acetic acid (4 drops per 250 mL)
- Oxalic acid, 2 % aqueous solution
- Sodium thiosulfate, 5 % aqueous solution

2.10.2. Procedure

1 Dewax (2 × 15 min xylene) and hydrate in descending concentrations of ethanol (4 min 96 %, 4 min 80 %, 4 min 70 %, 4 min 60 %, 2 × 5 min distilled water)
2 Stain in protargol S solution + copper sheet for 1 min 30 s at 55 °C (light-protected)
3 Wash in distilled water (3 × 30 s)
4 Reduce in hydrochinon solution for 10 min
5 Wash in lukewarm running tap water for 10 min
6 Wash in distilled water (2 × 10 s)
7 Incubate in intensifier for 3 min (light-protected)
8 Wash in distilled water (3 × 30 s)
9 Place in gold chloride solution for 3 min
10 Wash in distilled water (3 × 30 s)
11 Reduce in oxalic acid solution for 4 min
12 Wash in distilled water (3 × 30 s)
13 Place in sodium thiosulfate solution for 10 min
14 Wash in lukewarm running tap water for 5 min
15 Dehydrate slices (2 × 4 min 96 % ethanol, 4 min 2-propanol)
16 Clear in xylene (2 × 10 min) and mount in resinous medium (e.g. entellan)

2.11. Microscopy

Images were taken using a ZEISS microscope (Axio Lab.A1, Carl Zeiss Microscopy, Jena, Germany) equipped with a ZEISS Axiocam 105 color camera (Carl Zeiss Microscopy). Sections stained with picrosirius red were inspected by using crossed polarizing filters, additionally, they underwent fluorescence imaging on a ZEISS microscope (Axio Vert.A1, Carl Zeiss Microscopy) with the ZEISS Axiocam 503 color camera (Carl Zeiss Microscopy) and two different sets of filters (Table 1). Images with filters for green and red fluorescence in place were taken independently and digitally superimposed. ZEN software was used for microscopy and imaging (v 3.1, Carl Zeiss Microscopy).

3. Results

3.1. Fixation and demineralization

Preparation of an orifice through the dental hard tissues enabled immediate and adequate fixation of the pulpal tissue and thus prevented tissue degradation. Particularly the partial separation of crown and root allowed the connective pulpal tissue to shrink towards the adjacent dentine and thus avoided artefacts such as separation and tearing.

The series of radiographs facilitated qualitative monitoring the progress of demineralization, where a sharp front between decalcified and still calcified tissue was visible. Concomitant determination of sample weight enabled the quantification of the demineralization process.

While weight loss in samples treated with EDTA stagnated after 21 days indicating complete demineralization, samples in Morse's solution reached this point seven days earlier, after 14 days (Fig. 2a,b). The half-life of soluble compounds in single- and multi-rooted specimens in EDTA was 3.40 days and 3.02 days, respectively, whereas decalcification in Morse's solution reduced the half-life period to 1.39 and 1.72 days, respectively. In accordance with these findings, radiographic assessment revealed that calcification had disappeared after 7 days (single-rooted teeth) and 14 days (multi-rooted teeth) in Morse's solution and after 14 days (single-rooted teeth) and 28 days (multi-rooted teeth) in EDTA (Fig. 2c,d).

3.2. Hematoxylin-eosin staining

3.2.1. Stained elements of the dentine-pulp-complex

- blue: cell nuclei, bacteria
- red: cytoplasm, collagen fibres (in pulpal connective tissue and dentine), erythrocytes

Hematoxylin-eosin staining of the pulpal tissue in crown and root provides a detailed view of the characteristics of the healthy pulp-dentine-complex (Fig. 3). The coronal pulp exhibits a layer of numerous odontoblasts with elongated (columnar) and superimposed cell bodies (Fig. 3a,b), whereas fewer and cube-shaped odontoblasts in a palisade-like arrangement appear in the radicular pulp (Fig. 3c,d). Blood vessels cross the connective tissue (Fig. 3c). The layer of predentine appears paler compared to dentine, albeit with a low contrast between them. A purple hue inside the dentinal tubules indicates the invasion of bacteria in a caries-affected sample, however, the staining method does not allow for a differentiation of bacteria species (Fig. 3e).

The hematoxylin-eosin staining provides an excellent overview of the anatomical structures of the tooth, without specifically highlighting particular cell types or tissues.

3.3. Masson trichrome staining

3.3.1. Stained elements of the dentine-pulp-complex

- dark red: cell nuclei
- pale red: cytoplasm
- azure or bright red: collagen fibres (in pulpal connective tissue and dentine)

Fig. 4a,b illustrates Masson trichrome staining of a healthy tooth. The collagenous matrix of dentine appears in azure, displaying its tubular structure. The pulp shows its characteristic cell types and layers. In particular, Masson trichrome shows the fibrous texture of the pulp's extracellular matrix, and blood vessels can be recognized clearly due to the dark colour of the cells lining the vessels as well as the erythrocytes within. Applied to a carious tooth with pulp necrosis (Fig. 4c), the decay of dentine can be visualized, along with the different morphologies of primary and reactionary dentine with a distinct border between them (Fig. 4d). Dentine shows high affinity to aniline blue, but also to scarlet-acid fuchsine and thus appears either in azure or in bright red.

The Masson trichrome staining complements the hematoxylin-eosin staining for a comprehensive overview of the pulp with its cellular components, the extracellular matrix as well as the structure of the adjacent dentine.

3.4. Masson-Goldner trichrome staining

3.4.1. Stained elements of the dentin-pulp-complex

- blue-black: cell nuclei
- slightly red: cytoplasm
- red: erythrocytes

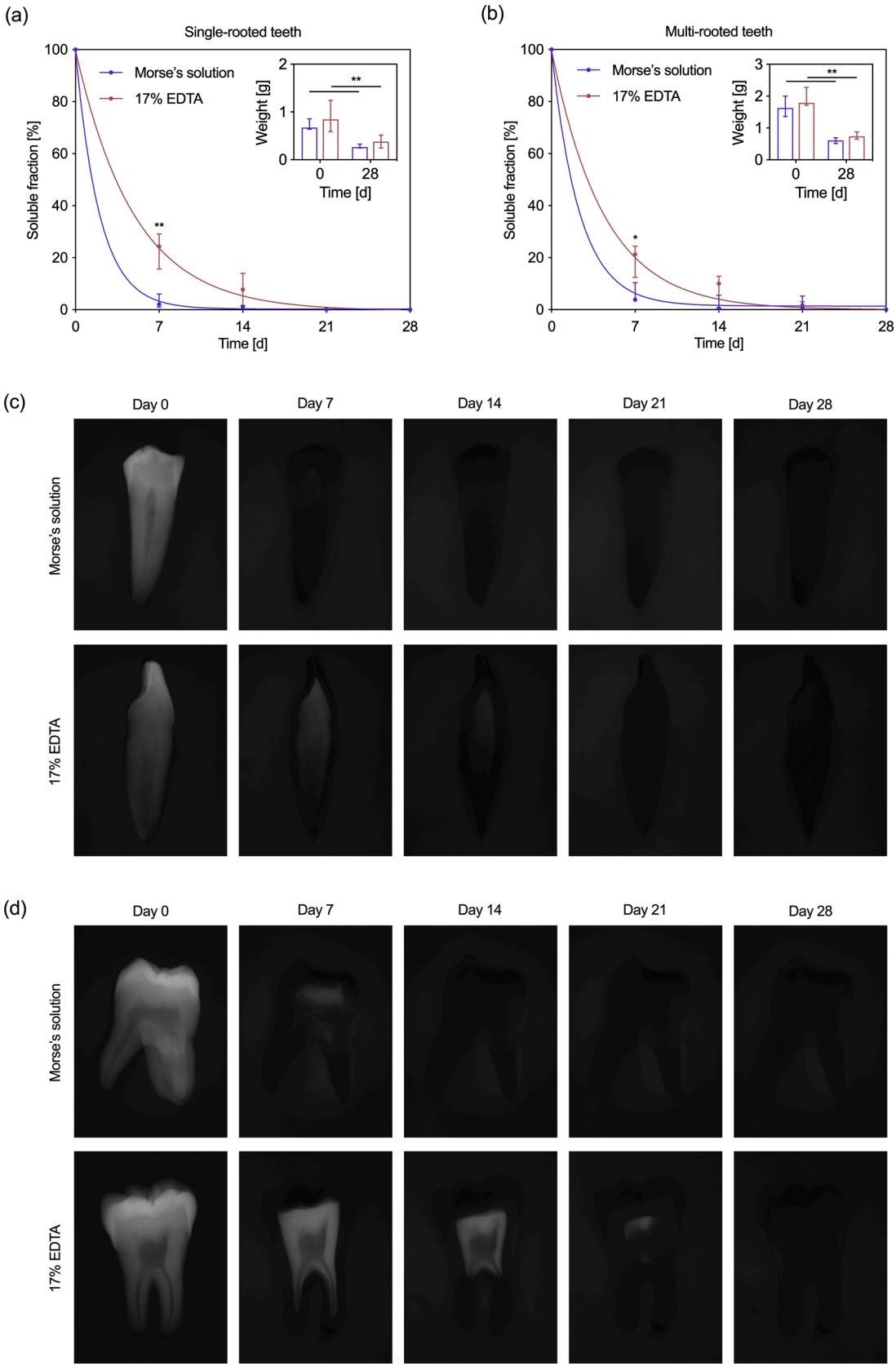

Fig. 2. Monitoring of the demineralization by EDTA and Morse's solution. (a,b) Weight loss of single and multi-rooted teeth over a decalcification period of 28 days. (c,d) Radiographs of healthy teeth show continuous demineralization over 28 days.

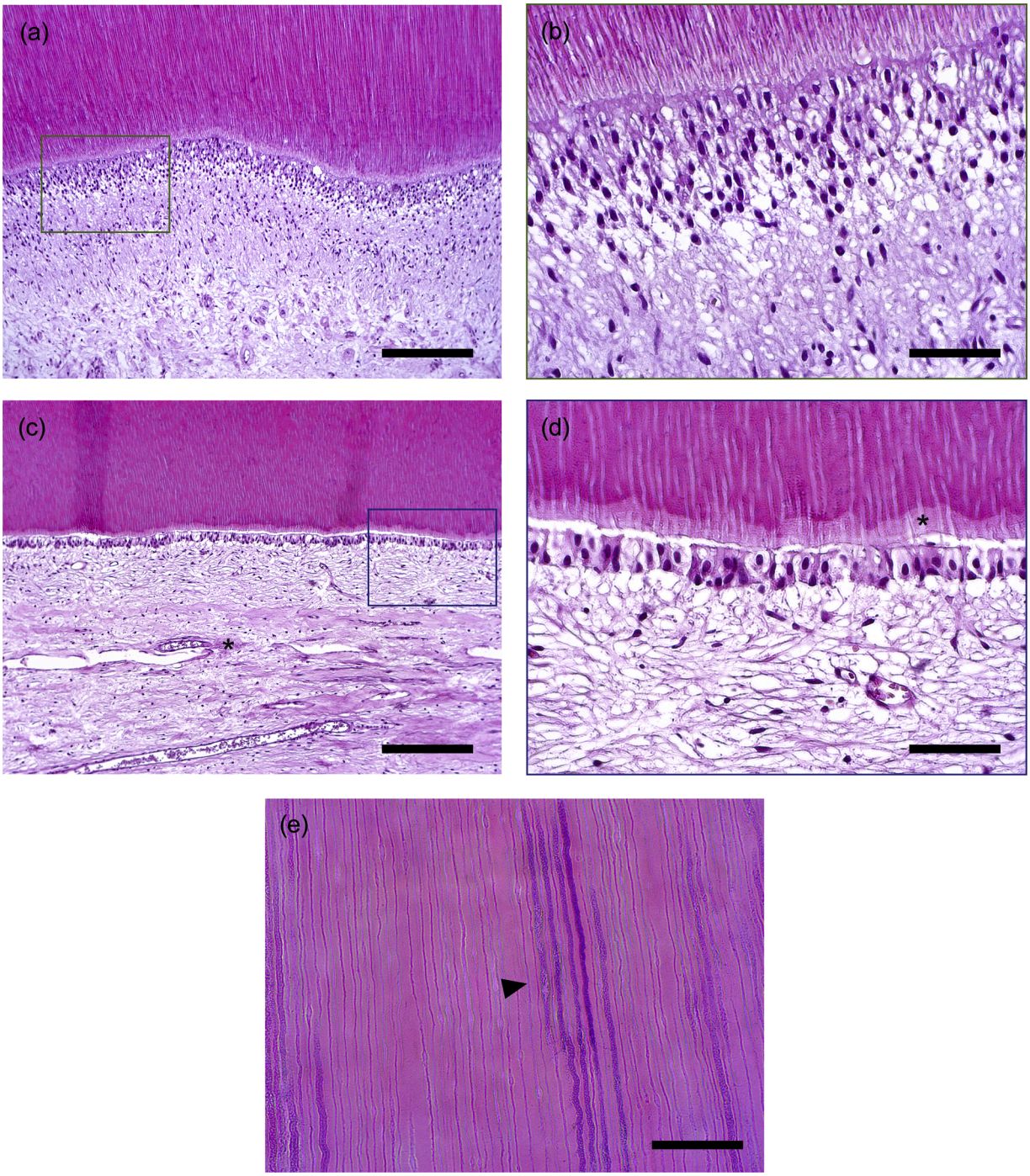

Fig. 3. Hematoxylin-eosin staining. Overview of a coronal pulp (a) with odontoblasts in multiple rows (b) and radicular pulp (c) with a single layer of odontoblasts (d). Radicular pulp (c) shows the typical bundle of blood vessels (asterisk). A magnified view of the dentine-pulp-interface (d) reveals the predentine, which shows a paler shade of pink and can thus be distinguished from previously mineralized dentine (asterisk). Bacteria that colonize the dentinal tubules can be observed in a carious tooth (arrowhead). Boxes in (a) and (c) represent views of (b) and (d). Scale bars: 200 μm (a,c), 50 μm (b,d,e). (For interpretation of the references to colour in this figure text, the reader is referred to the web version of this article.)

- green/red: collagen fibres (in pulpal connective tissue, dentine and osseous tissue)

Whereas the Masson-Goldner trichrome staining displays the characteristic components of the pulp-dentine-complex, it is particularly suitable with regard to vascular wall structures, especially the sub-odontoblastic capillaries appear rich in contrast (Fig. 5a). Fig. 5b and c show the pathological process of inflammatory root resorption. Multinuclear odontoclastic cells dig resorption lacunae into the dentine surface (Fig. 5b). As the resorption progresses, the degradation of mineralized tissue occurs alongside the apposition of new tissue, leading to the deposition of an entrapped osseous reparative tissue, which can be clearly differentiated by structure and colour after Masson-Goldner trichrome staining (Fig. 5c).

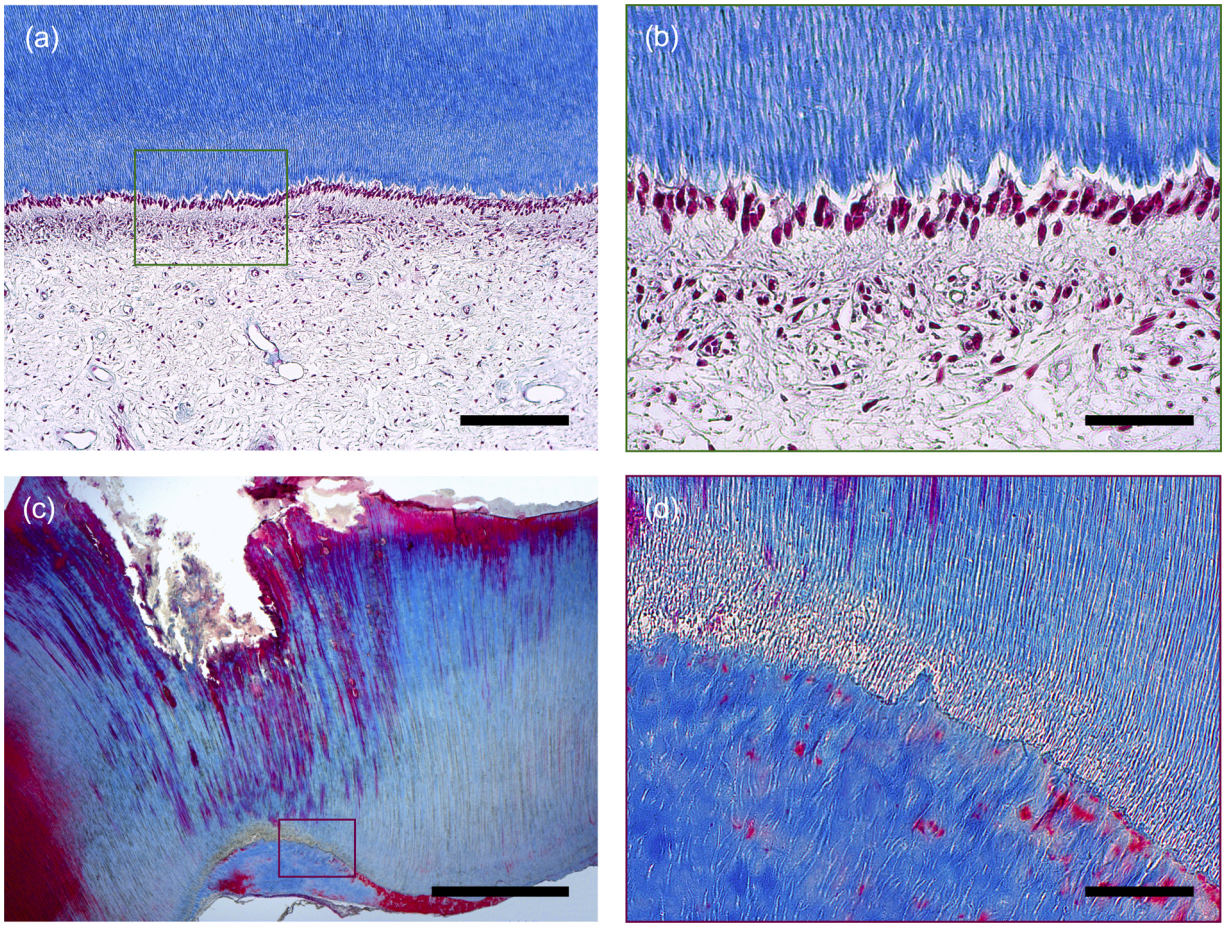

Fig. 4. Masson trichrome staining. (a) Overview of the different cell types and areas in a healthy tooth: odontoblast layer, subodontoblast layer devoid of cells, cell-rich zone, pulp core with blood vessels. (b) Detailed view of the dentine-pulp-interface with odontoblasts that extend their processes into the tubules. (c) Tooth with a carious lesion and pulp necrosis. (d) Detailed view of the boundary between secondary and tertiary dentine. Secondary dentine with parallel regular dentinal tubules. Tertiary dentine with fewer, irregularly shaped dentinal tubules, a high density of collagen and metachromasy. The transition area exhibits tissue structure of lower density. Boxes in (a) and (c) represent views of (b) and (d). Scale bars: 200 μm (a), 50 μm (b), 1000 μm (c), 100 μm (d). (For interpretation of the references to colour in this figure text, the reader is referred to the web version of this article.)

3.5. TRAP staining

3.5.1. Stained elements of the dentine-pulp-complex

- bright pink: odontoclasts
- pale purple: cell nuclei
- pale rose: dentine, extracellular matrix

Fig. 5d shows enzyme histochemical TRAP staining applied to a tooth with inflammatory root resorption. Clearly visible is the jagged dentine surface with clastic cells present in a resorption lacuna. This staining method sets out odontoclasts in bright pink against the surrounding structures in pale purple and rose.

3.6. Picrosirius red staining

3.6.1. Stained elements of the dentine-pulp-complex with non-polarized light

- grey/brown: cell nuclei
- yellow: cytoplasm, background
- bright red: collagen fibres (in pulpal connective tissue and dentine)

3.6.2. Stained elements of the dentine-pulp-complex with polarized light

- yellow-orange birefringence: collagen fibres in predentine and mineralized dentine, perivascular
- green birefringence: collagen fibres in tertiary dentine and pulpal connective tissue
- dark: background and non-collagenous structures

3.6.3. Stained elements of the dentine-pulp-complex with fluorescence filters

- red fluorescence: collagen (in pulpal connective tissue and dentine)
- green autofluorescence: cell nuclei, erythrocytes
- dark: background

Fig. 6 shows a healthy molar (Fig. 6a,c,e) and a carious premolar with extensive reactionary dentinogenesis (Fig. 6b,d,f) after picrosirius red staining. Sections were examined using non-polarized light (Fig. 6a, b), polarized light (6c,d) and with fluorescence filters, displaying the tissue's (auto)fluorescence (Fig. 6e,f).

In general, this staining method presents collagen fibres in an intense red colour. Examination of the sections through crossed polars reveals the fibrous structure of collagen more clearly and with high contrast against a dark background. The predentine appears brighter due to its non-mineralized collagenous structure compared to the (originally)

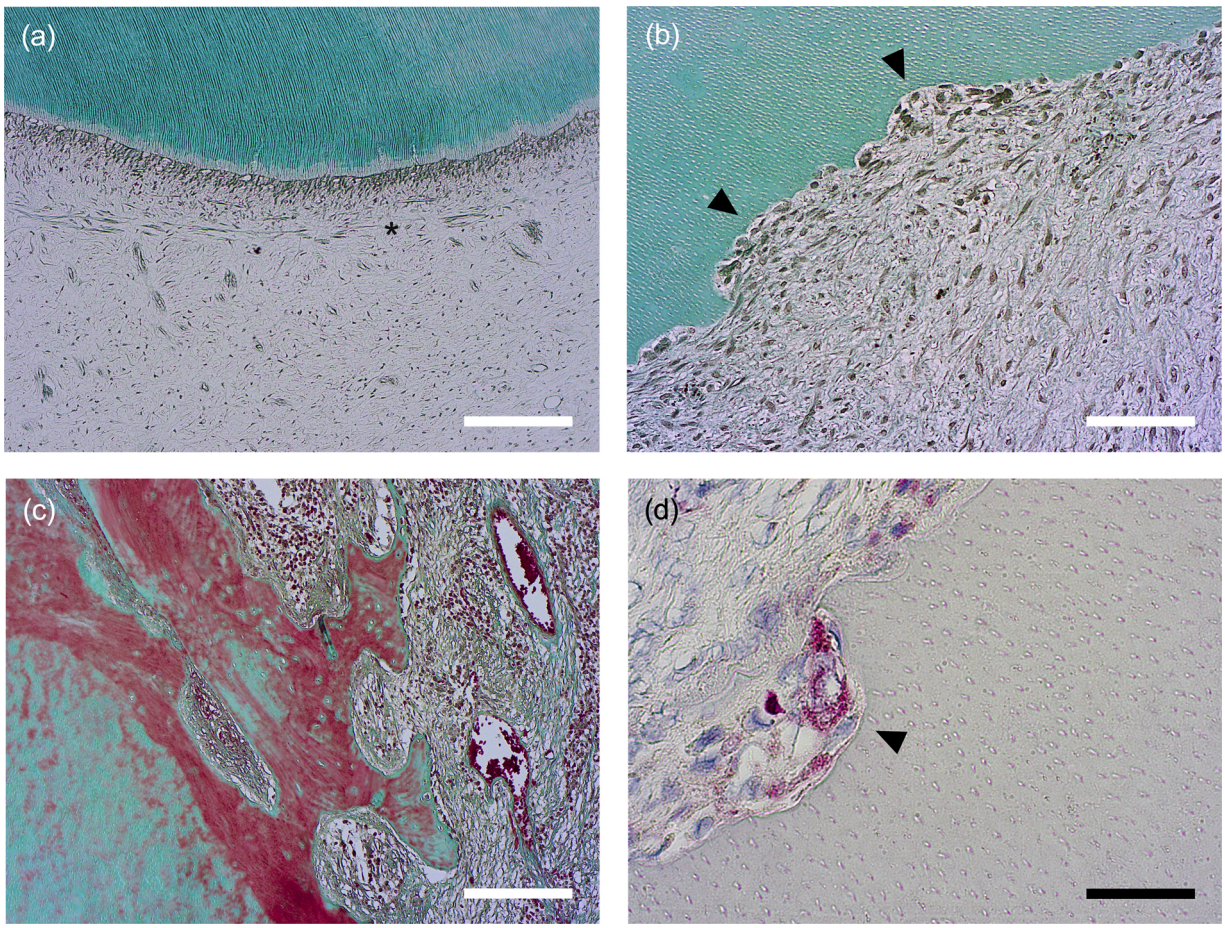

Fig. 5. Masson-Goldner trichrome staining (a-c) and TRAP staining (d). (a) Typical anatomy of coronal pulp tissue with subodontoblast capillaries (asterisk). (b) Tooth with external root resorption and resorption lacunae in dentine (arrowheads). (c) Inflammatory resorptive tissue with dilated vessels and abundance of leucocytes, remodelling of dentine by bone-like hard tissue. (d) Specific TRAP staining of clastic cells, so called odontoclasts. Scale bars: 200 μm (a,c), 100 μm (b), 50 μm (d). (For interpretation of the references to colour in this figure text, the reader is referred to the web version of this article.)

mineralized dentine, both displaying the typical tubular architecture. The cell-rich odontoblast layer impresses as a dark area due to its lack of collagen, whereas beneath, the collagenous network of the pulp's extracellular matrix is faintly visible (Fig. 6c). The reactionary dentine of the carious tooth appears irregular in structure and rich in collagen as indicated by its birefringence, which can clearly be distinguished from the regularly formed tubular dentine (Fig. 6d).

The (auto)fluorescent properties of the dentine-pulp complex permits the visualization of collagen fibres in the red colour spectrum, and cell nuclei as well as erythrocytes in the green spectrum. Thus, the structure of the odontoblast cell bodies is precisely visible in bright green, as are erythrocytes entrapped in blood vessels (Fig. 6e). The structures of the extracellular matrix and collagen emerge in bright red (Fig. 6e) with much higher clarity compared to the visualization with polarized light (Fig. 6c). At the interface between secondary and tertiary dentine, cellular inclusions emerge from the surrounding collagen (Fig. 6f).

Picrosirius red staining with the various imaging techniques allows visualization of collagen fibres, in particular their structure, orientation and density within dental hard and soft tissues in high resolution and clarity.

3.7. Modified Brown and Brenn staining

3.7.1. Stained elements of the pulp-dentine-complex

- blue: gram-positive bacteria
- red: gram-negative bacteria
- yellow: other tissue components

The bacteria that invade the dentinal tubules and penetrate towards the pulp chamber are clearly visible in red, blue and purple in a carious tooth (Fig. 7). It has to be noted that both crystal violet and basic fuchsine also precipitate unspecifically, resulting in a weak staining of dentine areas that were free of bacteria (Fig. 7a). Higher magnification reveals a specific coloration of bacteria in dentinal tubules and collaterals (Fig. 7b,c). However, the exact differentiation between gram-positive and gram-negative bacteria is difficult due to superimposition.

3.8. May-Gruenwald-Giemsa staining

3.8.1. Stained elements of the dentine-pulp-complex

- violet: cell nuclei, bacteria
- blue: cytoplasm
- light rose: background, dentine

This type of staining visualizes the structure of different types of dentine, which allows for a clear distinction between secondary and tertiary dentine. In addition, bacteria that are present in the dentinal tubules can be noticed by a dark blue or purple colour (Fig. 8a). The specimen of a carious tooth displays inflamed pulpal tissue at a late stage of degradation, indicated by disintegrating cells, dilated blood vessels and large vacuoles (Fig. 8b,c). The staining does not allow for a reliable

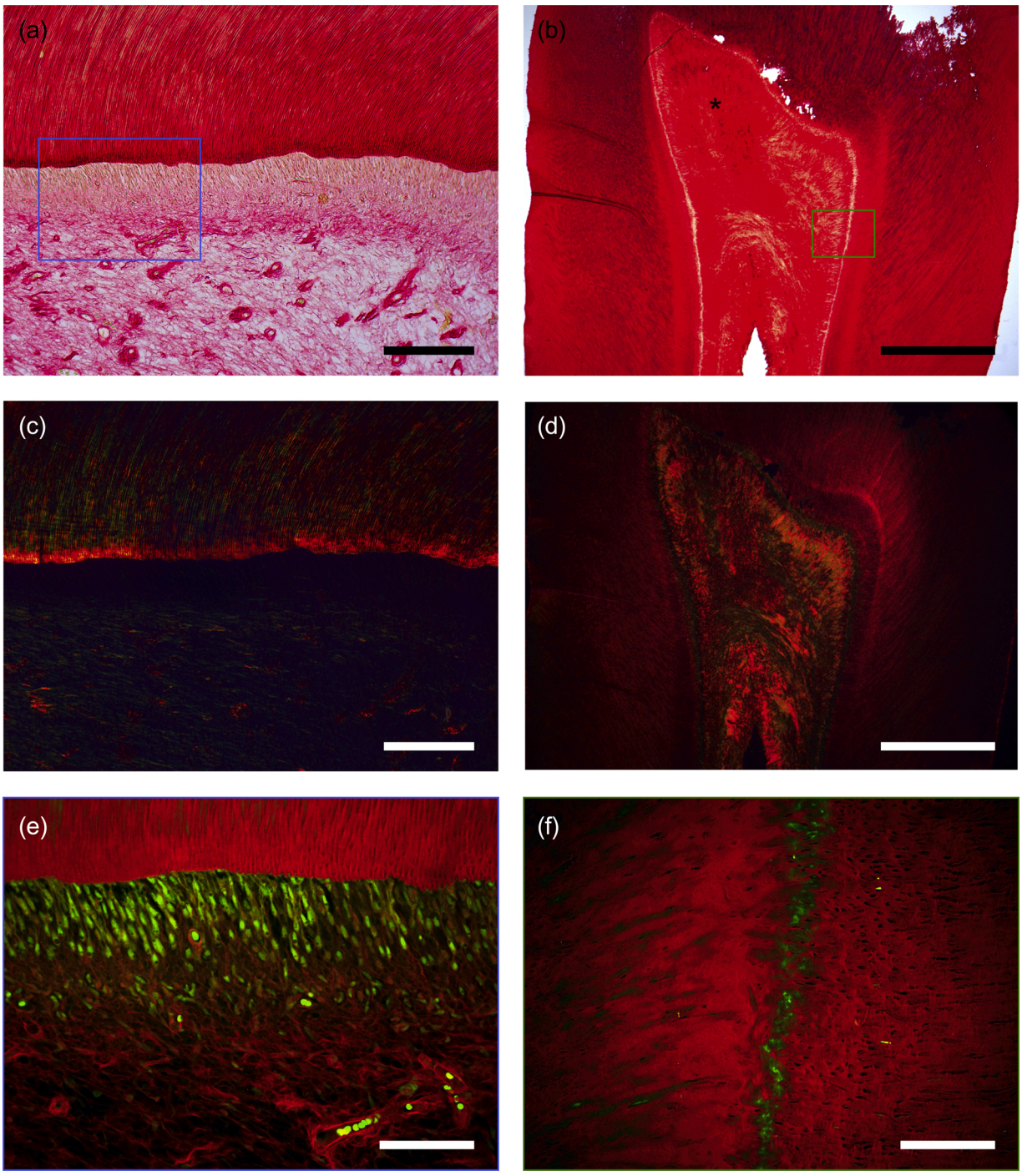

Fig. 6. Picrosirius red staining. (a) The dentine-pulp-interface with unpolarized light shows a low density of collagen in the odontoblast layer, but a high density in the vessel walls and predentine. (b) Imaging of regular and reactionary dentine (asterisk) in a carious tooth reveals a high collagen density in the dental hard tissues with structural differences among the dentine types. (c) With crossed polars, particularly the predentine appears rich in collagen whereas the odontoblast layer appears black. (d) No clear boundary between regular and reactionary dentine can be observed with polarized light. Less structured reactionary dentine contains a high density of collagen fibres, especially with green birefringence. (e) Detailed view of the odontoblast layer using the (auto)fluorescent properties of the stained tissue. Whereas cell nuclei and erythrocytes appear green-fluorescent, red fluorescence indicates collagen fibres. (f) At the interface between tubular dentine and unstructured reactionary dentine, green autofluorescence indicates inclusion of cellular components. Boxes in (a) and (b) represent views in (e) and (f). Scale bars: 200 μm (a,c), 1000 μm (b,d), 50 μm (e), 100 μm (f). (For interpretation of the references to colour in this figure text, the reader is referred to the web version of this article.)

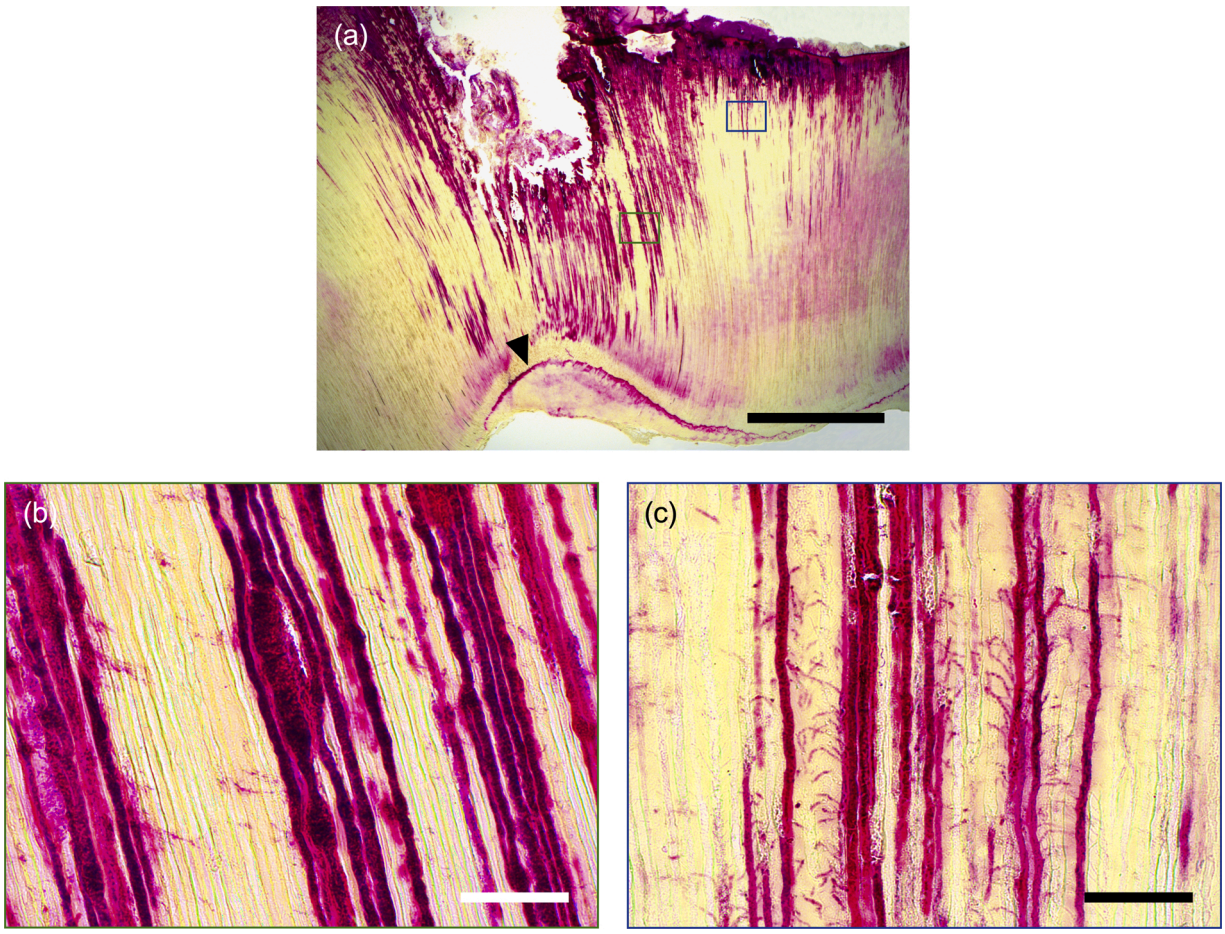

Fig. 7. Modified Brown and Brenn staining. (a) Overview of a carious lesion with bacterial biofilm colonizing the lesion and invading the dentinal tubules toward the pulp chamber. A precipitation of dye can be observed at the boundary between regular and reactionary dentin (arrow) above the pulp chamber. (b) Magnified view of bacterial invasion along the dentinal tubules forming ampulla-shaped dilations. (c) Bacteria also colonized the collateral connection between the main tubules. Boxes in (a) represent views of (b) and (c). Scale bars: 1000 μm (a), 50 μm (b,c). (For interpretation of the references to colour in this figure text, the reader is referred to the web version of this article.)

differentiation between different cell types such as pulp and immune cells.

3.9. Luxol fast blue staining

3.9.1. Stained elements of the dentine-pulp-complex

- dark blue: cell nuclei
- turquoise: dentine, myelin sheaths
- grey: extracellular matrix

The luxol fast blue staining applied to a healthy tooth clearly visualizes pulpal nerve fibres by staining the myelin sheaths in turquoise (Fig. 9a). The odontoblast layer and also the dentine show a high affinity to the dyes, where predentine can be distinguished from regular dentine by its lighter colour.

3.10. Bodian silver staining

3.10.1. Stained elements of the dentine-pulp-complex

- dark grey to black: nerve fibres, cell nuclei
- light grey: collagen fibres
- light purple to grey: dentine

Bodian staining of a healthy tooth turned out to be weak and low in contrast, however, nerve fibres were clearly displayed and were set apart from the grey background of the pulpal fibroblasts and extracellular matrix (Fig. 9b).

4. Discussion

Due to their complex structure and intimate association of different soft and mineralized tissues, human teeth raise particular challenges for histological processing, in every step of the procedure from fixation to demineralization, sectioning and staining. Thus, the main goal of this work was to optimize histological staining methods particularly with regards to their applicability and relevance to dental tissues, to precisely note down the laboratory procedures and to provide a compilation of useful protocols for dental researchers. All staining techniques were applied to both sound and carious or otherwise diseased teeth and evaluated regarding their potential strengths and weaknesses.

Histological methods have been used for the longest time, and certainly they have lost most of their previous significance due to the development of multiple analytical tools, mainly emerging from the fields of molecular biology or immunology. As we are used to analyse our samples with high precision by means of the latest technologies, it may be worthwhile to revisit these traditional techniques in combination with modern imaging tools. Thus, histology can add value to our work and give us a deeper understanding of the tissue architecture and

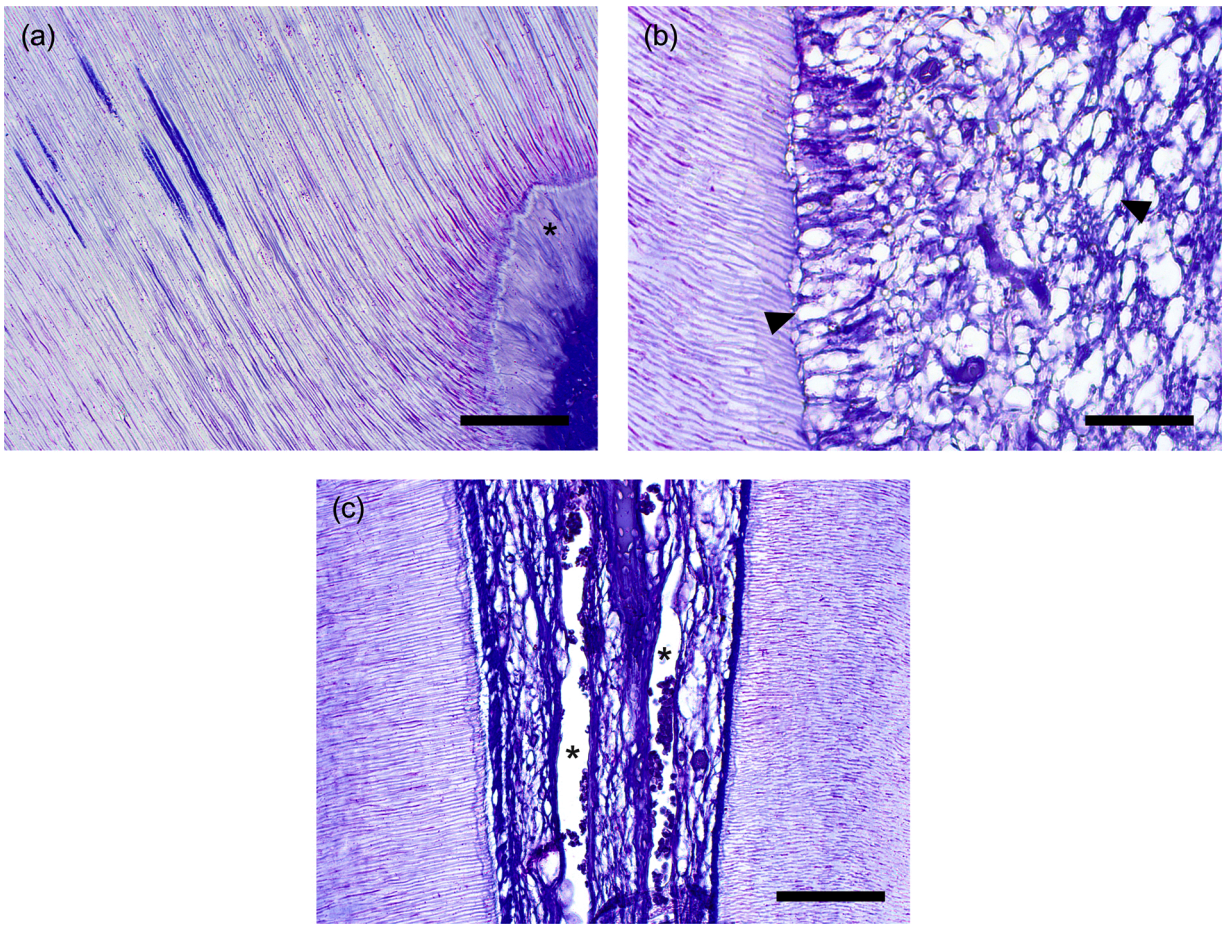

Fig. 8. May-Gruenwald-Giemsa staining. (a) Bacteria colonizing the dentinal tubules induce the formation of reactionary dentine; a gradual loss of tubular structure can be observed (asterisk). (b) Detailed view of vacuole-shaped changes in the odontoblastic and subodontoblastic layer of inflamed pulp tissue (arrowheads). (c) View of radicular pulp with degradative changes in tissue structure, abundance and dilaceration of vessels (asterisks). Scale bars: 100 μm (a,c), 50 μm (b). (For interpretation of the references to colour in this figure text, the reader is referred to the web version of this article.)

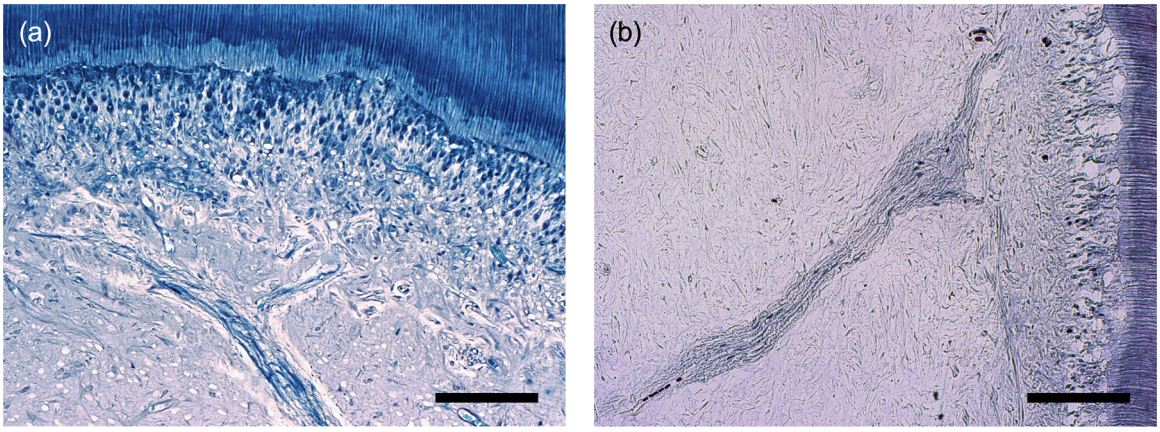

Fig. 9. Neuronal staining of healthy teeth. (a) In luxol fast blue staining, dentine can be clearly differentiated from predentine. A bundle of corrugated nerve fibres arborizes in the peripheral pulp tissue. (b) Staining according to Bodian reveals nerve fibres and accompanying vessels with high contrast. Scale bars: 100 μm (a,b). (For interpretation of the references to colour in this figure text, the reader is referred to the web version of this article.)

function and how it changes with disease. Although histological procedures are easy to conduct in principle, the devil is often in the details.

4.1. Fixation and demineralization

Particularly for teeth, a rapid fixation is essential to prevent degeneration and autolysis of the tissue during further processing. As hard dentine and enamel surround the dental pulp and impede the penetration of the fixing solution (Morse, 1945) except for teeth with incomplete root formation, the preparation of an artificial access seems essential for the sufficient diffusion of formaldehyde (Willman, 1937). The temperature of the fixative influences both the required duration as

well as tissue shrinkage (Fox et al., 1985). For teeth, the immersion in 4 % formaldehyde solution for 24 h at room temperature (20 °C) results in adequate fixation. As aldehyde fixation induces protein cross-linking (Thavarajah et al., 2012), it causes a distortion and thus shrinkage of the affected tissues, which may be different in soft and mineralized tissues. Thus, extended fixation should be avoided, however, most of the shrinkage observed on histological sections can be attributed to the numerous processing steps that follow (Fox et al., 1985). Subsequent to fixation, demineralization is necessary to enable sectioning of paraffin-embedded samples. Enamel, which consists nearly entirely of inorganic compounds (Brudevold et al., 1960), disappears completely. Dentine retains its shape after decalcification due to its organic matrix, mainly made of collagen fibres, which remain intact after decalcification (Tjäderhane et al., 2009). The demineralization agent should be chosen depending on the staining method to be performed. Acidic agents such as Morse's solution enable rapid decalcification, but may affect proteins and antigens, which has to be considered a potential pitfall for immunohistochemistry or enzyme histochemical staining. EDTA, a chelating agent is more gentle to the sample but requires more time (Cho et al., 2010). Independent of the choice of demineralizing agent, the exposure period should not be extended unnecessarily as it is associated with a risk of protein degradation and tissue destruction. Radiographic evaluation as a non-invasive method proved to be helpful in defining the endpoint of de calcification and reduce damage (Taqi et al., 2018), thus test-sectioning at various time points during demineralization was not necessary.

With paraffin-embedded sections, the loss of enamel is inevitable. If hard tissues are of interest, resin-embedding combined with sawing or grinding techniques can be applied. Fewer sections will be produced due to the width of the saw blade and subsequent grinding, but also because hard tissue sections require certain thickness for stability. Histologic staining methods are possible, but sectioning is technically more demanding (Donath & Breuner, 1982). However, hard tissue sections are not subject of this paper.

4.2. Hematoxylin-eosin staining

Hematoxylin-eosin staining is commonly used for routine histology (Hajj Hussein et al., 2015) and can be considered as technically simple. The first component, hemalaun, is aluminium-mordanted hematein, an oxidation product of hematoxylin (Llewellyn, 2009), which stains nuclear chromatin blue-purple. Eosin as its counterstaining visualizes red blood cells, collagen and smooth muscle tissue in different shades of pink (Feldman & Wolfe, 2014). Their combination provides a reasonable overview of the tissue structures and cellular microanatomy. In teeth, dentine and pulp stain due to their collagenous content. Images produced for this study are in line with descriptions of pulp tissue in the literature (Goldberg, 2014), in particular the pseudostratified order of odontoblasts in the coronal pulp and their single layer organization in the radicular pulp (Couve et al., 2013).

4.3. Trichrome staining

For trichrome staining techniques according to Masson or Masson-Goldner, three dyes are applied, where the third dye usually serves the purpose of counterstaining. For Masson staining, the collagen is stained by Biebrich scarlet-acid fuchsin and the tissue is counterstained by aniline blue. In the Masson-Goldner version, the collagen stain is acid fuchsine - ponceau azophloxine and the counterstain is light green. The staining is based on the ionic attachment of the acid dyes to amino groups, the unstained area is dyed by the counterstain (Llewellyn, 2008). Both methods revealed an inconstant affinity to collagen, which was highly sample-dependent. One reason for this variability may be that the affinity to collagen depends on the tension of collagen fibres, as described by Flint et al. for dermal and tendon tissue (Flint et al., 1975). Arylmethan dyes such as aniline blue and light green were more likely to stain tensioned collagen fibres. Disordered and atonic fibres with low affinity to the counterstains appeared to be located in the areas of dentine that were degraded by caries, but also in irregular dentine and predentine. Furthermore, preparation steps such as fixation and decalcification may have an impact, but it was not possible to draw valid conclusions during this study.

The properties of tertiary dentine, which forms e.g. in response to caries, provides information about the caries progression. Slowly progressing lesions allow the pulp to respond with the formation of regular tubular dentine by odontoblasts (reactionary dentine), whereas rapidly progressing lesions result in the hasty deposition of atubular and unstructured dentine (reparative dentine) (Bjørndal, 2001; Cooper et al., 2010). Reactionary dentine is formed by primary odontoblasts, reparative dentine is more likely formed by odontoblast-like cells, which differentiate from progenitor cells after the loss of primary odontoblasts (Smith & Cooper, 2015). It is possible to distinguish these two different types of dentine, apart from transitional forms, which may be deposited as soon as an active carious lesion changes to a more slowly progressing lesion (Bjørndal & Darvann, 1999). Besides effects of carious lesions, the degradation of dentine by resorptive processes was visualized histologically for this study. In general, resorptive processes can be characterized by odontoclasts, resorption lacunae, inflammatory processes and bone-like repair tissue (Mavridou et al., 2016). These typical features were shown using the Masson-Goldner staining technique. The differential visualization of osseous tissue and dentine was possible because of a higher affinity of the former toward acidic dyes, which may be due to a higher content of collagen and thus a higher number of available amino groups are available to bind to the dye (Fig. 5a–c).

4.4. TRAP staining

TRAP stands for tartrate-resistant acid phosphatase, an enzyme that can be detected in osteoclasts, macrophages, dendritic cells and in a variety of other cell types (Hayman, 2008). The TRAP staining solution contains naphthol AS-MX phosphate sodium salt which acts as an enzyme substrate. Therefore, the prerequisite for this enzyme histochemical staining is an intact catabolic centre after tissue processing and embedding (Willbold & Witte, 2010). The secretion of tartrate-resistant phosphatase by osteoclasts correlates with their resorptive behaviour (Kirstein et al., 2006). If observations are transferred to the histological investigations on odontoclasts from this study, it can be assumed that the TRAP concentration in these cells is also related to their resorptive activity. The stained odontoclasts are consequently involved in an active resorption process (Fig. 5d).

4.5. Picrosirius red staining

The picrosirius red dye attaches to collagen molecules and enhances the birefringence of the fibres. Microscopic imaging between crossed polarization filters allows a selective visualization of different collagen fibre strands (Junqueira et al., 1979). However, the ability of the picrosirius red staining and polarization microscopy to differentiate between collagen types by colour shades (type I: yellow, orange or red; type II: variable colour depending on tissue or species; type III: green) is discussed controversially (Junqueira, Cossermelli, & Brentani, 1978; Lattouf et al., 2014).

Predentine appears to contain a high density of collagen in polarization microscopy, as described in the literature (Frank & Nalbandian, 1989). Furthermore, the high number of odontoblasts formed a layer attached to dentine with reduced density of collagen.

In fluorescence microscopy, the picrosirius red dye gave red fluorescence signals, which were not present in unstained sections. By using respective filters, collagen showed red fluorescence and cells emit fluorescence in the green spectrum. The green autofluorescence might be traced back to lipofuscin (Vogel et al., 2015), which accumulates in post-mitotic cells such as odontoblasts (Gao et al., 1994). Green

Table 2
Schematic assessment of the different types of staining in regard to their ability to present specific anatomic structures. Hematoxylin-eosin staining (HE), Masson trichrome staining (MA), Masson-Goldner trichrome staining (GO), TRAP staining (TR), picrosirius red staining with light polarization (PS) and (auto)fluorescence (FL), modified Brown and Brenn staining (BB), May-Gruenwald-Giemsa staining (MG), luxol fast blue staining (LU) and Bodian silver staining (BO). Good (+), moderate (0) or weak (-).

	HE	MA	GO	TR	PS	FL	BB	MG	LU	BO
Microanatomy	+	+	+	–	–	+	–	+	0	–
Collagen fibres	–	+	+	–	+	+	–	+	0	–
Cell perceptibility	+	+	+	–	–	–	–	+	–	–
Bacteria	0	–	–	–	–	–	+	0	–	–
Nerve fibres	–	–	–	–	–	–	–	–	+	+
Clastic cells	–	–	–	+	–	–	–	–	–	–
Reproducibility	+	0	0	+	+	+	0	0	+	0

autofluorescence was also observed at the interface between secondary and tertiary dentine, which may be attributed to residual cells that were encapsulated during reparative dentinogenesis.

4.6. Modified Brown and Brenn staining

Carious lesions are characterized by a mixed infection and a biofilm composition that varies among individuals and even lesions. Furthermore, lesions in enamel and in dentine harbour different bacterial consortia, e.g. enamel lesions are dominated by *Streptococci*, whereas *Lactobacilli* are almost exclusively found in dentine lesions (Simón-Soro et al., 2014).

The original Brown and Brenn method modified by Taylor aims at the differential staining of bacteria in tissue sections (Dee Taylor, 1966). Gram-positive bacteria with their rigid, mucopeptide-containing layer are more likely to retain the primary stain, crystal violet. The stain is mordanted using iodine-potassium iodide to prevent decolorization and stabilize the stain (Biswas et al., 1970). As revisiting this technique showed, the most delicate step is the differentiation, which should selectively decolourize the gram-negative bacteria before counterstaining the tissue with basic fuchsine. This step is error-prone; however, more reproducible results were obtained by using an acetone-ethanol mixture. Overall, the incubation times of all different steps had to be adjusted individually for each sample.

Whereas bacteria within the carious lesion were stained reproducibly (Fig. 7a–c), they could not be differentiated consistently in gram positive and negative. The staining protocol has several problematic steps and is not suitable to stain different bacterial species reliably (Engbaek et al., 1979). Nevertheless, the intensity and localization of the infection were visualized, which is related to caries-induced tissue destruction and bacterial accumulation (Beltrame et al., 2012).

4.7. May-Gruenwald-Giemsa staining

The May-Gruenwald-Giemsa staining was originally developed for the differential staining of cells in blood smears. The goal was to adapt this method for histology in order to visualize inflammation and invading immune cells in tissue samples.

Instead of a differentiated representation of cytoplasm, cell nuclei, erythrocytes and different granules in colour and saturation, we observed a bluish tint over the whole section. The falsified staining result can be due to pH elevation (Binder et al., 2012), although the protocol was modified accordingly and the sections were neutralized by phosphate buffer. Furthermore, formaldehyde fixation can affect the staining outcome by increasing basophilia (Horobin, 2011). Nevertheless, it was possible to depict a inflammatory response in the pulp tissue. Bacterial antigens initiate the invasion of neutrophils and macrophages followed by cells of the specific immune response like T- and B-lymphocytes, which accumulate in the inflamed pulp tissue (Farges et al., 2015). Furthermore, a reduced number of odontoblasts and a disorganization of their palisading order was observed in carious teeth as described in previous studies (Lee et al., 2006). For a correct evaluation of the sections, it must be considered that one single section can show different stages of the pulp's inflammation depending on its location and direction within the tissue (Langeland, 1987). It has to be assumed that the most severe image most likely describes the actual state of the pulp.

4.8. Nerve fiber stainings: Luxol fast blue staining and Bodian silver staining

The dental pulp is innervated by afferent trigeminal nerve fibres with myelinated and non-myelinated axons, which transduce nociceptive signals. The associated Schwann cells are, apart from their myelinating function, involved in the regulation of immunological processes (Couve & Schmachtenberg, 2018). The difficulty of a histological visualization of neuronal structures lies in the fibre orientation - these need to be aligned in the sectional plane in order to be displayed properly.

Two staining procedures with different approaches were revisited in this study. Whereas the luxol fast blue staining only marks the myelinated fibres, the silver impregnation according to Bodian stains all neuronal elements of the pulp tissue (Fearnhead & Linder, 1956). The luxol fast blue staining protocol described by Kluever and Barrera is based on a structural similarity of the luxol fast blue and naturally occurring porphyrins in the myelin sheath, which allows for the attachment of the dye (Clasen et al., 1973) to myelinated nerve fibres ramified in the subodontoblastic layer, also known as plexus of Raschkow (Pashley et al., 2002). The silver impregnation stains all nervous elements in decalcified sections of teeth (Fearnhead & Linder, 1956). Bodian silver staining is based on impregnation of neurofilament polypeptides by silver proteinate (Gambetti et al., 1981). Subsequently, the silver proteinate is reduced to elemental silver by hydrochinone (Bodian, 1936). Despite the staining result was intensified using a silver intensifier based on silver nitrate, differentiation of gracile structures with this method appears limited (Katz & Watson, 1985). Arwill et al. combined neurophysiological measurements and histological observations in cat teeth (Arwill et al., 1973) and were able to show that nerve fibres infiltrate the odontoblast layer and the inner parts of the dentine. Classical histological staining displays the dental nervous tissue arborizing in the subodontoblastic layer, however, the evaluation of extra-pulpal spreading of nerval tissue was not possible due to insufficient colour contrast. Additional immunohistochemical methods are necessary to provide a detailed view of nerve fibre spreading into the dentine (Couve et al., 2018).

5. Conclusion

In conclusion, each of the staining methods possesses strengths and weaknesses to visualize anatomy, collagen fibres, cell differentiation, bacteria and nerve fibres as summarized in Table 2. Depending on the research question, a skilful combination of selected methods makes it possible to analyse dental tissues to a large extent. Finally, traditional histological techniques remain indispensable in modern research due to

their reproducibility, practicability and comparatively low cost. However, more comprehensive methods such as immunohistochemistry or molecular techniques can be used to complement traditional methods and to show specific structures or antigens.

Author contributions

M. Widbiller: supervision, conceptualization, writing - original draft, methodology; C. Rothmaier: conceptualization, writing - original draft, methodology, investigation; D. Saliter: methodology, investigation; M. Wölflick: methodology, investigation; A. Rosendahl: methodology, investigation; W. Buchalla: supervision, writing – review & editing; G. Schmalz: writing – review & editing; T. Spruss: writing – review & editing; K. M. Galler: supervision, conceptualization, writing original draft

Declaration of Competing Interest

The authors report no declarations of interest.

Appendix A. Supplementary data

Supplementary material related to this article can be found, in the online version, at doi:https://doi.org/10.1016/j.archoralbio.2021.105136.

References

Arwill, T., Edwall, L., Lilja, J., Olgart, L., & Svensson, S. E. (1973). Ultrastructure of nerves in the dentinal-pulp border zone after sensory and autonomic nerve transection in the cat. *Acta Odontologica Scandinavica, 31*(5), 273–281.

Beltrame, A. P., Bolan, M., Serratine, A. C., & Rocha, M. J. (2012). Bacterial intensity and localization in primary molars with caries disease. *Journal of the Indian Society of Pedodontics and Preventive Dentistry, 30*(1), 32–40.

Binder, T., Diem, H., Fuchs, R., Gutensohn, K., & Nebe, T. (2012). Pappenheim stain: Description of a hematological standard stain – History, chemistry, procedure, artifacts and problem solutions. *Laboratoriumsmedizin, 36*(5).

Biswas, B. B., Basu, P. S., & Pal, M. K. (1970). Gram staining and its molecular mechanism. *International Review of Cytology, 29*, 1–27.

Bjørndal, L. (2001). Presence or absence of tertiary dentinogenesis in relation to caries progression. *Advances in Dental Research, 15*(1), 80–83.

Bjørndal, L., & Darvann, T. (1999). A light microscopic study of odontoblastic and non-odontoblastic cells involved in tertiary dentinogenesis in well-defined cavitated carious lesions. *Caries Research, 33*(1), 50–60.

Bodian, D. (1936). A new method for staining nerve fibers and nerve endings in mounted paraffin sections. *The Anatomical Record, 65*, 89–97.

Bracegirdle, B. (1977). The history of histology: A brief survey of sources. *History of Science, 15*(2), 77–101.

Brudevold, F., Steadman, L. T., & Smith, F. A. (1960). Inorganic and organic components of tooth structure. *Annals of the New York Academy of Sciences, 85*, 110–132.

Cho, A., Suzuki, S., Hatakeyama, J., Haruyama, N., & Kulkarni, A. B. (2010). A method for rapid demineralization of teeth and bones. *The Open Dentistry Journal, 4*, 223–229.

Clasen, R. A., Simon, R. G., Scott, R., Pandolfi, S., Laing, I., & Lesak, A. (1973). The staining of the myelin sheath by luxol dye techniques. *Journal of Neuropathology and Experimental Neurology, 32*(2), 271–283.

Cooper, P. R., Takahashi, Y., Graham, L. W., Simon, S., Imazato, S., & Smith, A. J. (2010). Inflammation-regeneration interplay in the dentine-pulp complex. *Journal of Dentistry, 38*(9), 687–697.

Couve, E., & Schmachtenberg, O. (2018). Schwann cell responses and plasticity in different dental pulp scenarios. *Frontiers in Cellular Neuroscience, 12*, 299.

Couve, E., Lovera, M., Suzuki, K., & Schmachtenberg, O. (2018). Schwann cell phenotype changes in aging human dental pulp. *Journal of Dental Research, 97*(3), 347–355.

Couve, E., Osorio, R., & Schmachtenberg, O. (2013). The amazing odontoblast: Activity, autophagy, and aging. *Journal of Dental Research, 92*(9), 765–772.

Dee Taylor, R. (1966). Modification of the Brown and Brenn gram stain for the differential staining of gram-positive and gram-negative bacteria in tissue sections. *American Journal of Clinical Pathology, 46*(4), 472–474.

Donath, K., & Breuner, G. (1982). A method for the study of undecalcified bones and teeth with attached soft tissues. The Säge-Schliff (sawing and grinding) technique. *Journal of Oral Pathology, 11*(4), 318–326.

Engbaek, K., Johansen, K. S., & Jensen, M. E. (1979). A new technique for gram staining paraffin-embedded tissue. *Journal of Clinical Pathology, 32*(2), 187–190.

England, M. C., Pellis, E. G., & Michanowicz, A. E. (1974). Histopathologic study of the effect of pulpal disease upon nerve fibers of the human dental pulp. *Oral Surgery, Oral Medicine, Oral Pathology, 38*(5), 783–790.

Farges, J.-C., Alliot-Licht, B., Renard, E., Ducret, M., Gaudin, A., Smith, A. J., & Cooper, P. R. (2015). Dental pulp defence and repair mechanisms in dental caries. *Mediators of Inflammation, 2015*, Article 230251.

Fearnhead, R. W., & Linder, J. E. (1956). Observations on the silver impregnation of nerve fibres in teeth. *Journal of Anatomy, 90*(2), 228–235.

Feldman, A. T., & Wolfe, D. (2014). Tissue processing and hematoxylin and eosin staining. *Methods in Molecular Biology, 1180*, 31–43.

Flint, M. H., Lyons, M. F., Meaney, M. F., & Williams, D. E. (1975). The Masson staining of collagen—An explanation of an apparent paradox. *The Histochemical Journal, 7*(6), 529–546.

Fox, C. H., Johnson, F. B., Whiting, J., & Roller, P. P. (1985). Formaldehyde fixation. *The Journal of Histochemistry and Cytochemistry, 33*(8), 845–853.

Frank, R. M., & Nalbandian, J. (1989). Structure and ultrastructure of dentine. In B. K. B. Berkovitz, A. Boyde, R. M. Frank, H. J. Höhling, B. J. Moxham, J. Nalbandian, & C. H. Tonge (Eds.), *Teeth. Handbook of microscopic anatomy*. Berlin, Heidelberg: Springer.

Fuenzalida, M., Illanes, J., Lemus, R., Guerrero, A., Oyarzún, A., Acuña, O., & Lemus, D. (1999). Microscopic and histochemical study of odontoclasts in physiologic resorption of teeth of the polyphyodont lizard liolaemus gravenhorsti. *Journal of Morphology, 242*(3), 295–309.

Gambetti, P., Gambetti, L. A., & Papasozomenos, S. C. (1981). Bodian's silver method stains neurofilament polypeptides. *Science, 213*(4515), 1521–1522.

Gao, G., Johansson, U., Rundquist, I., & Ollinger, K. (1994). Lipofuscin-induced autofluorescence of living neonatal rat cardiomyocytes in culture. *Mechanisms of Ageing and Development, 73*(1), 79–86.

Gest, H. (2004). The discovery of microorganisms by Robert Hooke and Antoni Van Leeuwenhoek, fellows of the Royal Society. *Notes and Records of the Royal Society of London, 58*(2), 187–201.

Goldberg, M. (2014). Pulp anatomy and characterization of pulp cells. In M. Goldberg (Ed.), *The dental pulp: Biology, pathology, and regenerative therapies*. Berlin, Heidelberg: Springer.

Hajj Hussein, I., Raad, M., Safa, R., Jurjus, R., & Jurjus, A. (2015). Once upon a microscopic slide: The story of histology. *Journal of Cytology & Histology, 6*, 377.

Hayman, A. R. (2008). Tartrate-resistant acid phosphatase (TRAP) and the osteoclast/immune cell dichotomy. *Autoimmunity, 41*(3), 218–223.

Horobin, R. W. (2011). How Romanowsky stains work and why they remain valuable. *Biotechnic & Histochemistry, 86*(1), 36–51.

Junqueira, L. C., Cossermelli, W., & Brentani, R. (1978). Differential staining of collagens type I, II and III by sirius red and polarization microscopy. *Archivum Histologicum Japonicum, 41*(3), 267–274.

Junqueira, L. C. U., Bignolas, G., & Brentani, R. R. (1979). Picrosirius staining plus polarization microscopy, a specific method for collagen detection in tissue sections. *The Histochemical Journal, 11*(4), 447–455.

Katele, K. V., & James, V. E. (1962). Innervation of the hamster maxillary incisor. *Journal of Dental Research, 41*, 1072–1084.

Katz, M. J., & Watson, L. F. (1985). Intensifier for Bodian staining of tissue sections and cell cultures. *Stain Technology, 60*(2), 81–87.

Kirstein, B., Chambers, T. J., & Fuller, K. (2006). Secretion of tartrate-resistant acid phosphatase by osteoclasts correlates with resorptive behavior. *Journal of Cellular Biochemistry, 98*(5), 1085–1094.

Lane, N. (2015). The unseen world: Reflections on Leeuwenhoek (1677) "concerning little animals". *Philosophical Transactions of the Royal Society of London. Series B, Biological Sciences, 370*(1666).

Langeland, K. (1987). Tissue response to dental caries. *Endodontics & Dental Traumatology, 3*(4), 149–171.

Lattouf, R., Younes, R., Lutomski, D., Naaman, N., Godeau, G., Senni, K., & Changotade, S. (2014). Picrosirius red staining: A useful tool to appraise collagen networks in normal and pathological tissues. *Journal of Histochemistry & Cytochemistry, 62*(10), 751–758.

Lee, Y.-L., Liu, J., Clarkson, B. H., Lin, C.-P., Godovikova, V., & Ritchie, H. H. (2006). Dentin-pulp complex responses to carious lesions. *Caries Research, 40*(3), 256–264.

Lennon, Á., Buchalla, W., Rassner, B., Becker, K., & Attin, T. (2006). Efficiency of 4 caries excavation methods compared. *Operative Dentistry, 31*(5), 551–555.

Llewellyn, B. (2008). Differential staining with acid dyes. *Presentation to the Queensland Histology Group at Caloundra*, 1–25.

Llewellyn, B. (2009). Nuclear staining with alum hematoxylin. *Biotechnic & Histochemistry, 84*(4), 159–177.

Mavridou, A. M., Hauben, E., Wevers, M., Schepers, E., Bergmans, L., & Lambrechts, P. (2016). Understanding external cervical resorption in vital teeth. *Journal of Endodontics, 42*(12), 1737–1751.

Mazzarello, P., Garbarino, C., & Calligaro, A. (2009). How Camillo Golgi became "the Golgi". *FEBS Letters, 583*(23), 3732–3737.

Morse, A. (1945). Formic acid-sodium citrate decalcification and butyl alcohol dehydration of teeth and bones for sectioning in paraffin. *Journal of Dental Research, 24*(3–4), 143–153.

Musumeci, G. (2014). Past, present and future: Overview on histology and histopathology. *Journal of Histology and Histopathology, 1*, 5.

Pashley, D. H., Walton, R. E., & Slavkin, H. C. (2002). Histology and physiology of the dental pulp. In J. I. Ingle, & L. K. Bakland (Eds.), *Endodontics*. Hamilton: BC Decker Inc.

Pereira, T., Dodal, S., & Tamgadge, A. (2014). Analysis of collagen fibres in human dental pulp using picrosirius red stain and polarised microscopy. *Journal of Pierre Fauchard Academy (India Section), 28*(3), 73–77.

Ricucci, D., Loghin, S., & Siqueira, J. F. (2014). Correlation between clinical and histologic pulp diagnoses. *Journal of Endodontics, 40*(12), 1932–1939.

Ricucci, D., Siqueira, J. F., Loghin, S., & Lin, L. M. (2017). Pulp and apical tissue response to deep caries in immature teeth: A histologic and histobacteriologic study. *Journal of Dentistry, 56*(Supplement C), 19–32.

Simón-Soro, A., Guillen-Navarro, M., & Mira, A. (2014). Metatranscriptomics reveals overall active bacterial composition in caries lesions. *Journal of Oral Microbiology, 6*, 25443.

Slaoui, M., & Fiette, L. (2011). Histopathology procedures: From tissue sampling to histopathological evaluation. *Methods in Molecular Biology, 691*, 69–82.

Smith, A., & Cooper, P. R. (2015). Cellular signaling in dentin repair and regeneration. In A. Vishwakarma, P. Sharpe, S. Shi, & M. Ramalingam (Eds.), *Stem cell biology and tissue engineering in dental sciences*. Boston: Academic Press.

Taqi, S. A., Sami, S. A., Sami, L. B., & Zaki, S. A. (2018). A review of artifacts in histopathology. *Journal of Oral and Maxillofacial Pathology, 22*(2), 279.

Thavarajah, R., Mudimbaimannar, V. K., Elizabeth, J., Rao, U. K., & Ranganathan, K. (2012). Chemical and physical basics of routine formaldehyde fixation. *Journal of Oral and Maxillofacial Pathology, 16*(3), 400–405.

Tjäderhane, L., Rocha Carrilho, M., Breschi, L., Tay, F., & Pashley, D. (2009). Dentin basic structure and composition—An overview. *Endodontic Topics, 20*.

Vogel, B., Siebert, H., Hofmann, U., & Frantz, S. (2015). Determination of collagen content within picrosirius red stained paraffin-embedded tissue sections using fluorescence microscopy. *MethodsX, 2*, 124–134.

Willbold, E., & Witte, F. (2010). Histology and research at the hard tissue–implant interface using Technovit 9100 New embedding technique. *Acta Biomaterialia, 6*(11), 4447–4455.

Willman, M. (1937). A technique for the preparation of histologic sections through teeth and jaws for teaching and research. *Journal of Dental Research, 16*, 183–190.

Wolters, W. J., Duncan, H. F., Tomson, P. L., Karim, I. E., McKenna, G., Dorri, M., … van der Sluis, L. W. M. (2017). Minimally invasive endodontics: A new diagnostic system for assessing pulpitis and subsequent treatment needs. *International Endodontic Journal, 50*(9), 825–829.